http://dx.doi.org/10.5012/bkcs.2012.33.3.906

# Poly(ethylenimine)-Stabilized Hollow Gold-Silver Bimetallic Nanoparticles: Fabrication and Catalytic Application†

**Kuan Soo Shin,* Ji Hoon Kim, In Hyun Kim, and Kwan Kim‡,***

*Department of Chemistry, Soongsil University, Seoul 156-743, Korea. *E-mail: kshin@ssu.ac.kr*
*‡Department of Chemistry, Seoul National University, Seoul 151-742, Korea. *E-mail: kwankim@snu.ac.kr*
*Received December 21, 2011, Accepted January 5, 2012*

Hollow gold-silver bimetallic nanoparticles (AuAg-HNPs) have been synthesized and their optical and structural properties were characterized. Initially Ag nanoparticles (Ag-NPs) were prepared using poly(ethylenimine) (PEI) as a reducing and a stabilizing agent simultaneously. AuAg-HNPs could then be synthesized *via* galvanic replacement reaction in a PEI aqueous solution by reacting sacrificial Ag template with a precursor compound of Au, i.e., $HAuCl_4$. Due to the presence of abundant amine functional groups in PEI, which could act as the dissolving ligand for AgCl, the precipitation problem of $Ag^+$ in the presence of Cl from $HAuCl_4$ salt was avoided. On this basis, the relatively high concentrations of $HAuCl_4$ and PEI-stabilized Ag nanoparticles could be used for the fabrication of AuAg-HNPs. Because of their increased surface areas and reduced densities, the AuAg-HNPs were expected and confirmed to outperform their solid counterparts in applications such as catalysis for the reduction of 4-nitrophenol in the presence of $NaBH_4$.

**Key Words :** Au-Ag, Hollow nanoparticles, Poly(ethylenimine), Catalyst, 4-Nitrophenol

## Introduction

Recently, many efforts have been made toward the synthesis of more complex structures, core-shell or hollow nanostructures. Due to their increased surface areas, reduced densities, and tunable surface plasmon resonance (SPR) characteristics,[1] hollow nanostructures are expected to surpass their solid counterparts in applications such as optical imaging,[2] surface-enhanced Raman scattering (SERS),[3] catalysis,[4] and photothermal therapy.[5] Xia and co-workers, who pioneered in this filed, have demonstrated that hollow nanostructures of various noble metals could be synthesized *via* galvanic replacement reaction in an aqueous solution by reacting sacrificial Ag template with a precursor compound of the desired metal such as Au, Pd, or Pt.[6-8] For a galvanic replacement reaction between Ag nanostructures and $HAuCl_4$ in an aqueous solution, however, the AgCl on the product side needed to be removed from the surface of the particles by refluxing the system utilizing the high solubility of AgCl in water at 100 °C.[7] Otherwise, the AgCl would precipitate out and prevent the formation of Au-Ag bimetallic hollow nanostructures with uniform, homogeneous walls.

Branched poly(ethylenimine) (PEI), which contains primary, secondary, and tertiary amino groups, has been known to be not only a cationic polymer used as a versatile vector for cell transfection[9] but also an efficient agent for the preparation of stabilized Au nanoparticles (Au-NPs).[10,11] The reductive capability of amines has been known for a long time, but the detailed mechanism of how Au-NPs are formed by amines has not yet been clarified. In the polyamine-based syntheses of nanoparticles, most of the works have been focused on the preparation of Au-NPs.[10-12] In contrast, surprisingly, not many works have been published on the synthesis of Ag or Au-Ag bimetallic nanoparticles using polyamine. Recently, we reported that PEI-stabilized Ag nanoparticles (Ag-NPs) were readily produced when a mixture of PEI and $AgNO_3$ solutions was heated. The size of the Ag-NPs was largely dependent on the molar ratio of PEI and $AgNO_3$: Increasing the molar ratio of PEI, smaller metal particles were produced, and vice versa.[13]

In this study, a new strategy to produce relatively high concentration of amine-stabilized Au-Ag bimetallic hollow nanoparticles (AuAg-HNPs) has been developed for the first time, to the best of our knowledge, *via* a PEI-assisted galvanic replacement process of Ag by Au. Due to the presence of abundant amine functional groups in PEI, which can act as the dissolving ligand for AgCl, the precipitation problem of $Ag^+$ in the presence of $Cl^-$ from the gold salt can be avoided.[14] Therefore, the relatively high concentrations of $HAuCl_4$ and PEI-stabilized Ag-NPs could be applied for the fabrication of the AuAg-HNPs. In addition, the as-prepared AuAg-HNPs have been exploited as efficient catalysts for the reduction of 4-nitrophenol in the presence of $NaBH_4$.

## Experimental

Hydrogen tetrachloroaurate ($HAuCl_4$, 99.99%), silver nitrate ($AgNO_3$, 99.8%), branched poly(ethylenimine) (PEI, MW ~60 kDa), sodium borohydride ($NaBH_4$, 99%), and 4-nitrophenol (99%) were purchased from Aldrich, and used as received. Other chemicals, unless specified, were reagent-grade, and highly purified water, with a resistivity greater than 18.0 MΩ · cm (Millipore Milli-Q System), was used in

†This paper is to commemorate Professor Kook Joe Shin's honourable retirement.

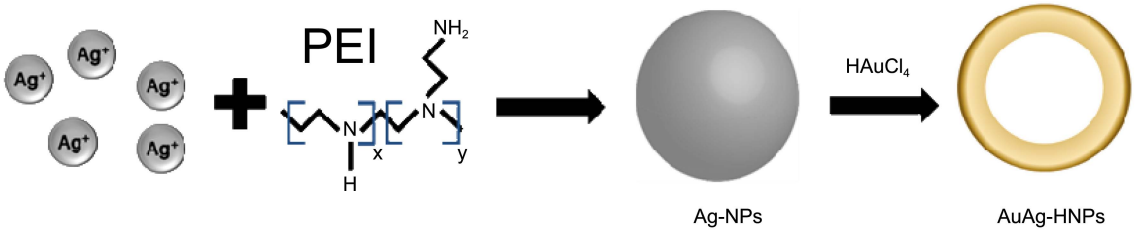


**Figure 1.** Schematic presentation of the preparation of AuAg-HNPs. (a) Ag-NPs were prepared using PEI as a reducing and a stabilizing agent simultaneously: (b) Aqueous $HAuCl_4$ solution was added dropwise to PEI-stabilized Ag-NPs solution: (c) AuAg-HNPs were produced *via* a PEI-assisted galvanic replacement process of Ag by Au.

preparing aqueous solutions. PEI-stabilized AuAg-HNPs could be synthesized *via* a galvanic replacement reaction. Initially Ag-NPs were prepared using PEI as a reducing and a stabilizing agent simultaneously. The PEI-capped Ag-NPs were synthesized by heating a mixture of 48.5 mL of 20 mM $AgNO_3$ and 1.5 mL of 2% (w/w) PEI for 60 min. AuAg-HNPs could then be synthesized *via* galvanic replacement reaction in an aqueous solution by reacting sacrificial Ag template with a precursor compound of Au. The 30 mL of 1 mM (atomic concentration) Ag-NPs sol was brought to reflux with stirring, and then 6 mL of 1.0 mM aqueous $HAuCl_4$ solution were added dropwise. The solution changed from brown to red-purple and, finally, to a deep blue color. Figure 1 shows a schematic representation of the preparation of AuAg-HNPs. Aqueous $HAuCl_4$ solution was added drop by drop to Ag-NPs solution prepared beforehand using PEI. AuAg-HNPs were then produced *via* a PEI-assisted galvanic replacement process of Ag by Au. For reference, PEI-capped Au-NPs were also prepared by heating a mixture of 50 mL of 1.5 mM aqueous $HAuCl_4$ solution and 0.4 mL of 2% (w/w) PEI for 30 min. In a typical catalytic reaction, 15 μL of 10 mM 4-nitrophenol and 30 μL of 0.1 mM (atomic concentration) Ag-NP, Au-NP, or AuAg-HNP sol were mixed with 2.6 mL of highly purified water at 25 °C in a poly(methyl methacrylate) cell. A fresh aqueous solution of 100 μL of 1.0 M $NaBH_4$ was then added with constant stirring, and UV-visible (UV-vis) absorption spectra were recorded with time to monitor the change in the reaction mixture. UV-vis absorption spectra were obtained using Avantes 3648 spectrometers. Energy-filtering transmission electron microscope (EF-TEM) images were taken on a LIBRA 120 model at 120 kV. Energy-dispersive X-ray spectroscopy (EDX) characterization was performed with a SUPRA 55VP Field-Emission Scanning Electron Microscope (FE-SEM) operating at 15 kV.

## Results and Discussion

The formation of Ag-NPs, Au-NPs, and AuAg-HNPs can be confirmed from the fact that only one SPR band appears in the optical absorption spectra of the sols in the as-prepared state (see Fig. 2). The SPR of metal nanostructures results from incident light being scattered and absorbed at a resonant frequency due to the collective oscillation of

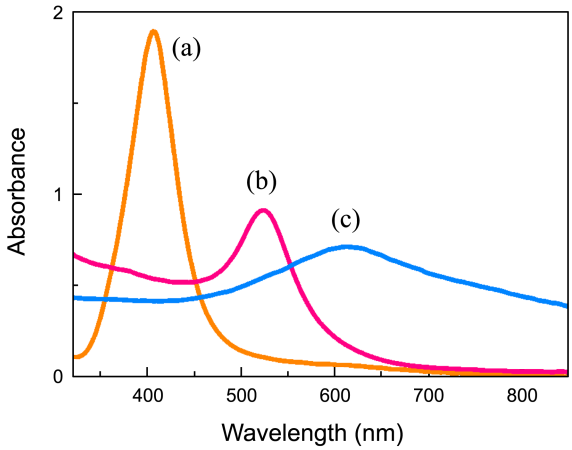


**Figure 2.** UV-vis absorption spectra of (a) Ag-NPs, (b) Au-NPs, and (c) AuAg-HNPs.

conduction electrons. The relative intensity of the scattering and absorption cross-sections of metal nanoparticles can be tuned by varying their content, size, and shape. As shown in Figure 2, the Ag-NP and Au-NP sols have plasmon absorption bands at around 400 and 520 nm, respectively.[15] On the other hand, the AuAg-HNPs show the maximum SPR band at around 620 nm. As mentioned previously, AuAg-HNPs were synthesized *via* a PEI-assisted galvanic replacement process in an aqueous solution by reacting sacrificial Ag-NPs template with a precursor compound of Au, *i.e.*, $HAuCl_4$. Regarding the preparation of AuAg-HNPs, the reduction potential of $AuCl_4$/Au (0.99 V *vs* SHE) is more positive than that of $Ag^+$/Ag (0.8 V *vs* SHE). Thus, PEI-capped Ag-NPs can serve as a template for reaction, being oxidized by $HAuCl_4$ according to

$$3Ag(s) + HAuCl_4(aq) \rightarrow Au(s) + 3AgCl(s) + HCl(aq)$$

When the galvanic replacement reaction is carried out in an aqueous solution at high temperature, the replacement from Ag to Au nanoparticles involves a number of processes including dissolution of the Ag template with generation of Au atoms, deposition of Au on the surface of the Ag template, growth of the Au nanoparticles around the dissolving Ag template, diffusion of Ag into the Au shell and formation of Au-Ag alloys and, finally, an Ag oxidization process accompanied by a morphological transformation to produce

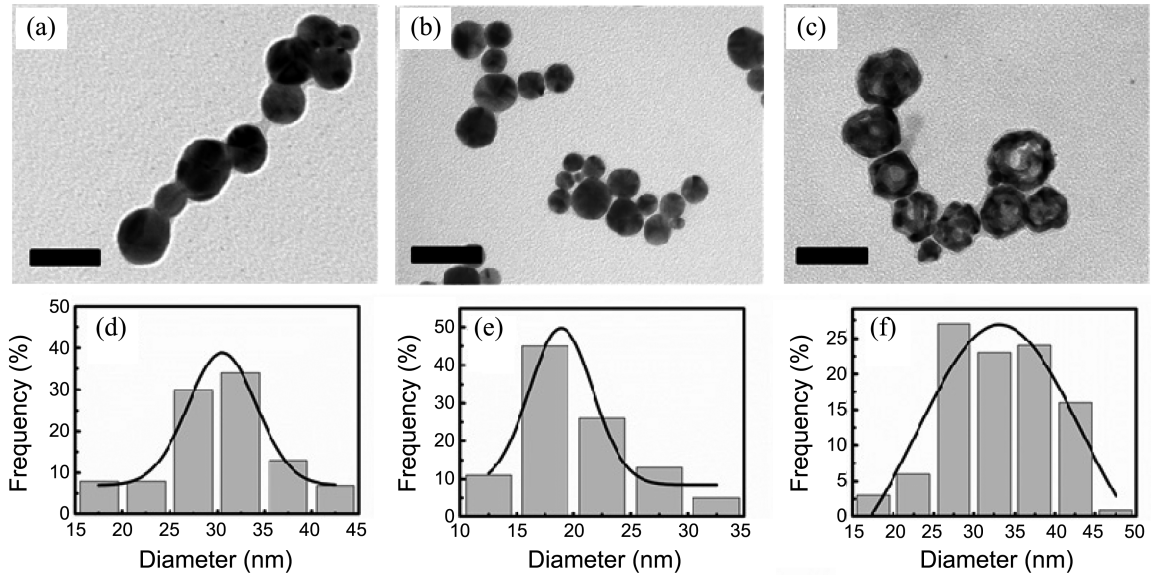


**Figure 3.** EF-TEM images of (a) Ag-NPs, (b) Au-NPs, and (c) AuAg-HNPs. (scale bar = 50 nm). Size distribution histograms of (d) Ag-NPs, (e) Au-NPs, and (f) AuAg-HNPs.

a hollow structure.[7]

To characterize the nanoparticle size and structure using EF-TEM, a part from the water solution containing sol nanoparticles was ultrasonicated for 15 min. A single micro-drop of the solution was allowed to dry on a carbon-coated copper grid for EF-TEM imaging. Figures 3(a)-(c) show the EF-TEM images of the Ag-NPs, Au-NPs, and AuAg-HNPs, respectively. The nanoparticles are all spherical in shape. The size distributions of the corresponding nanoparticles are shown as histograms in the Figures 3(d)-(f): The average sizes are measured to be 30.4 ± 6.3 nm, 20.4 ± 5.2 nm, and 33.0 ± 6.6 nm (with 5.7 ± 1.2 nm wall thicknesses) for Ag-NPs, Au-NPs, and AuAg-HNPs, respectively. The atomic composition of AuAg-HNPs was determined from the EDX analysis (see Figure 4): The Au-to-Ag ratio in AuAg-HNPs was estimated to be 38 : 62.

In order to investigate the catalytic activity of the AuAg-HNPs, we have chosen the reduction of 4-nitrophenol by $NaBH_4$ as a model reaction. Indeed, many research groups have investigated the reduction of 4-nitrophenol using a number of noble metal nanoparticles, such as Au, Ag and Cu, as catalysts.[16-20] Here, three different Ag-NPs, Au-NPs, and AuAg-HNPs were used on the catalytic reduction of 4-nitrophenol in the presence of $NaBH_4$. It has been observed that, after immediate addition of freshly prepared aqueous solution of $NaBH_4$, the peak due to 4-nitrophenol was red shifted from 317 to 400 nm as shown in Figure 5(a). This peak was due to the formation of 4-nitrophenolate ions in alkaline condition caused by the addition of $NaBH_4$.[17] In the absence of proper catalyst, the thermodynamically favorable reduction of 4-nitrophenol (the standard reduction potentials for 4-nitrophenol/4-aminophenol and $H_3BO_3/BH_4^-$ are −0.76 and −1.33 V, respectively) was not observed and the peak due to 4-nitrophenol ions at 400 nm remains unaltered even a couple of days as reported in the literatures.[16]

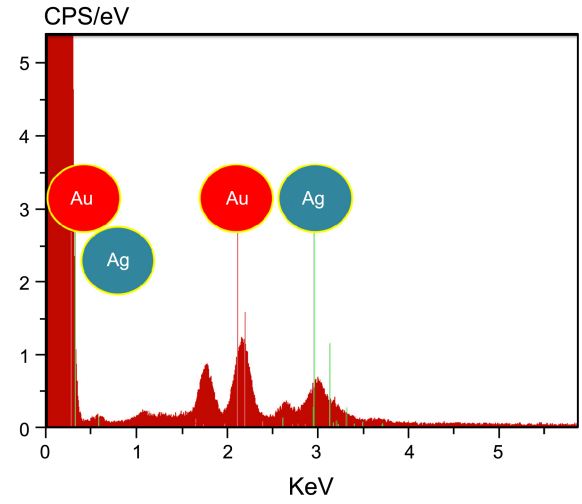


**Figure 4.** EDX spectrum of AuAg-HNPs.

The rapid catalytic conversion of the 4-nitrophenol to 4-aminophenol after addition of AuAg-HNPs samples was quantitatively monitored as a successive decrease in the peak height at 400 nm (see Fig. 5(b)) and the gradual development of the new peak at 300 nm which substantiates the formation of the 4-aminophenol,[20] corresponding to a change in solution color from light yellow to yellow-green. In this experiment, the concentration of the borohydride ion, used as reductant, largely exceeds that of 4-nitrophenol. As soon as we added the $NaBH_4$, the AuAg-HNPs started the catalytic reduction by relaying electrons from the donor $BH_4^-$ to the acceptor 4-nitrophenol right after the adsorption of both onto the particle surfaces. As the initial concentration of sodium borohydride was very high, it remained essentially constant throughout the reaction. For the evaluation of the catalytic rate, the pseudo-first-order kinetics with respect to 4-

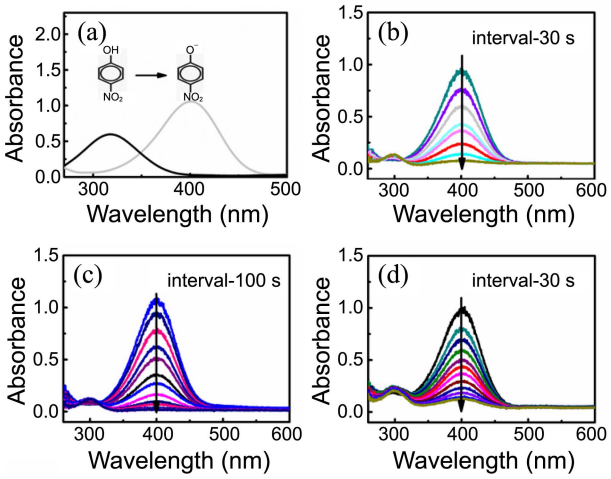


**Figure 5.** (a) UV-vis absorption spectra of 4-nitrophenol taken before (*black*) and after (*gray*) immediate addition of $NaBH_4$. Successive UV-vis absorption spectra taken after adding $NaBH_4$ into 4-nitrophenol solution in the presence of (b) AuAg-HNPs, (c) Ag-NPs, and (d) Au-NPs. The arrows are a visual guide to show the direction of spectral changes with time.

nitrophenol will then be a reasonable assumption. In this light, since the ratio of absorbance $A_t$ of 4-nitrophenol at time $t$ to its value $A_0$ measured at $t = 0$ must be equal to the concentration ratio $C_t/C_0$ of 4-nitrophenol, the kinetic equation for the reduction can be written as

$$dC_t/dt = -k_{app}C_t \text{ or } \ln(C_t/C_0) = \ln(A_t/A_0) = -k_{app}t$$

where $C_t$ is the concentration of 4-nitrophenol at time $t$ and $k_{app}$ is the apparent rate constant, which can be obtained from the decrease of the peak intensity at 400 nm with time.

Figures 5(c) and 5(d) show the representative UV-vis spectra of the catalytic reduction of 4-nitrophenol into 4-aminophenol using the Ag-NPs and Au-NPs, respectively, in the presence of $NaBH_4$. In these catalytic reactions, a good linear fitting of $\ln(A_t/A_0)$ versus the reaction time was also obtained, indicating that pseudo-first-order kinetics could be used to calculate the kinetic rate constant. A good linear correlation, $\ln(A_t/A_0)$ versus time, is obtained for all the systems studied as demonstrated in Figure 6(a). The kinetic rate constants of the Ag-NPs, Au-NPs, as well as AuAg-HNPs are estimated in Figure 6(b). The rate constant of AuAg-HNPs was $9.2 \pm 1.7 \times 10^{-3}$ $s^{-1}$, which is significantly higher than those of Ag-NPs and Au-NPs, ($2.8 \pm 0.73 \times 10^{-3}$ and $6.4 \pm 1.5 \times 10^{-3}$ $s^{-1}$ for Ag-NPs and Au-NPs, respectively): It needs to be noted that the total number of Au-NPs would be larger than those of Ag-NPs and AuAg-HNPs because the size of Au-NPs is smaller than those of Ag-NPs and AuAg-HNPs but the same atomic concentrations of Au-NPs, Ag-NPs, and AuAg-HNPs are applied during the catalytic reaction. Because of their increased surface areas and reduced densities, the AuAg-HNPs were expected and confirmed to outperform their solid counterparts in applications such as catalysis for the reduction of 4-nitrophenol in the presence of $NaBH_4$. This method of synthesis of the hollow nanoparticles stabilized by the positively charged PEI

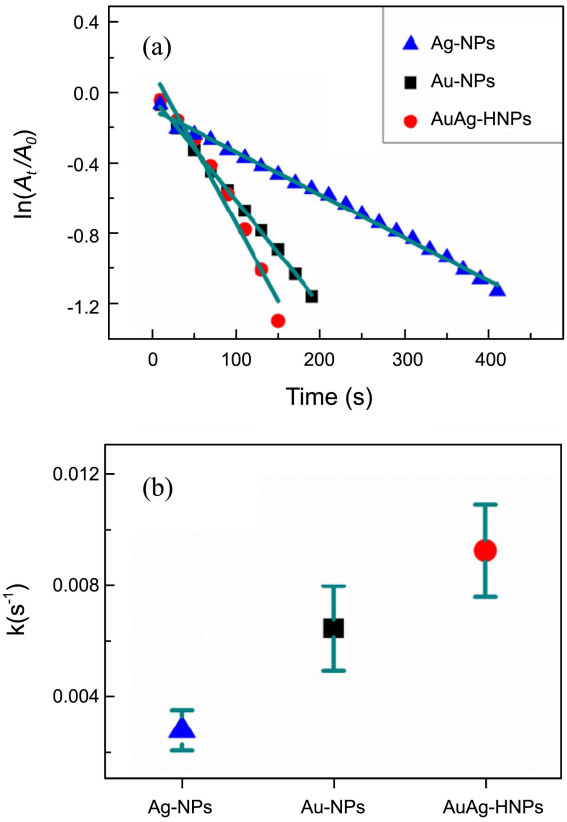


**Figure 6.** (a) Plot of $\ln(A_t/A_0)$ against reaction time for Ag-NPs, Au-NPs, and AuAg-HNPs and (b) rate constants for the Ag-NPs, Au-NPs, and AuAg-HNPs in the catalytic reduction of 4-nitrophenol in the presence of $NaBH_4$. The error bar indicates the standard deviation in 5 different measurements.

polymer may be suitable for designing several heterogeneous catalytic systems.

## Conclusions

In this investigation, a new strategy to produce relatively high concentration of PEI-stabilized AuAg-HNPs *via* a PEI-assisted galvanic replacement reaction has been developed. Initially Ag-NPs were prepared using PEI as a reducing and a stabilizing agent simultaneously. AuAg-HNPs could then be synthesized *via* galvanic replacement reaction in a PEI aqueous solution by reacting sacrificial Ag-NPs with $HAuCl_4$. Due to the presence of abundant amine functional groups in PEI, which could act as the dissolving ligand for AgCl, the precipitation problem of $Ag^+$ in the presence of $Cl^-$ from $HAuCl_4$ salt was avoided. Therefore, the relatively high concentrations of $HAuCl_4$ and Ag-NPs could be applied for the fabrication of the AuAg-HNPs. In order to investigate the catalytic activity of the AuAg-HNPs, we have chosen the reduction of 4-nitrophenol by $NaBH_4$ as a model reaction. In these catalytic reactions, a good linear fitting of $\ln(A_t/A_0)$ versus the reaction time was obtained, indicating that pseudo-first-order kinetics could be used to calculate the kinetic rate constant. The rate constant of AuAg-HNPs was significantly higher than those of Ag-NPs and Au-NPs

probably due to their increased surface areas and reduced densities.

**Acknowledgments.** This work was supported by National Research Foundation (NRF) of Korea Grant funded by the Korean Government (MEST) (No. 2011-0001218, 2011-0006737, 2011-0019157, and 2009-0072467).

## References

1. Selvakannan, P. R.; Sastry, M. *Chem. Comm.* **2005**, 1684.
2. Shukla, S.; Priscilla, A.; Banerjee, M.; Bhonde, R. R.; Ghatak, J.; Satyam, P. V.; Sastry, M. *Chem. Mater.* **2005**, *17*, 5000.
3. Schwartzberg, A. M.; Oshiro, T. Y.; Zhang, J. Z.; Huser, T.; Talley, C. E. *Anal. Chem.* **2006**, *78*, 4732.
4. Yang, J.; Lee, J.Y.; Too, H. P.; Valiyaveettil, S. *J. Phys. Chem. B* **2006**, *110*, 125.
5. Zhang, J. Z. *J. Phys. Chem. Lett.* **2010**, *1*, 686.
6. Chen, J.; McLellan, J. M.; Siekkinen, A.; Xiong, Y.; Li, Z. Y.; Xia, Y. *J. Am. Chem. Soc.* **2006**, *128*, 14776.
7. Sun, Y.; Xia, Y. *J. Am. Chem. Soc.* **2004**, *126*, 3892.
8. Chen, J.; Wiley, B.; McLellan, J.; Xiong, Y.; Li, Z. Y.; Xia, Y. *Nano Lett.* **2005**, *5*, 2058.
9. Godbey, W. T.; Wu, K. K.; Mikos, A. G. *Proc. Natl. Acad. Sci. U S A* **1999**, *96*, 5177.
10. Sun, X.; Dong, S.; Wang, E. *Mater. Chem. Phys.* **2006**, *96*, 29.
11. Kim, K.; Lee, H. B.; Lee, J. W.; Park, H. K.; Shin, K. S. *Langmuir* **2008**, *24*, 7178.
12. Sun, X.; Dong, S.; Wang, E. *Langmuir* **2005**, *21*, 4710.
13. Kim, K.; Lee, H. B.; Lee, J. W.; Shin, K. S. *J. Colloid Interface Sci.* **2010**, *345*, 103.
14. Shin, K. S.; Kim, J. H. *Bull. Korean Chem. Soc.* **2011**, *32*, 2469.
15. Lee, P. C.; Meisel, D. *J. Phys. Chem.* **1982**, *86*, 3391.
16. Hayakawa, K.; Tomokazu, Y.; Esumi, K. *Langmuir* **2003**, *19*, 5517.
17. Lee, K. Y.; Lee, Y. W.; Lee, J. H.; Han, S. W. *Colloid Surf. A* **2010**, *372*, 146.
18. Patra, A. K.; Dutta, A.; Bhaumik, A. *Catal. Comm.* **2010**, *11*, 651.
19. Shin, Y.; Dohnalkova, A.; Lin, Y. *J. Phys. Chem. C* **2010**, *114*, 5985.
20. Rashid, Md. H.; Bhattacharjee, R. R.; Kotal, A.; Mandal, T. K. *Langmuir* **2006**, *22*, 7141.